PHYSICAL REVIEW D **83,** 114045 (2011)

Exploring anomalous top-quark interactions via the final lepton in $t\bar{t}$ productions/decays at hadron colliders

Zenrō Hioki*

Institute of Theoretical Physics, University of Tokushima, Tokushima 770-8502, Japan

Kazumasa Ohkuma†

Department of Information Science, Fukui University of Technology, Fukui 910-8505, Japan

(Received 13 April 2011; published 23 June 2011)

We study momentum distributions of the final-state charged lepton in $p\bar{p}/pp \to t\bar{t} \to \ell^+ X(\ell = e \text{ or } \mu)$ at hadron colliders, i.e., Tevatron and Large Hadron Collider (LHC), in order to explore possible new-physics effects in the top-quark sector. Assuming general model-independent $t\bar{t}g + t\bar{t}gg$ and tbW interactions beyond the standard model, we first derive analytical formulas for the corresponding parton-parton processes. We then compute the lepton angular, energy, and transverse-momentum distributions in $p\bar{p}/pp$ collisions to clarify how they are affected by those anomalous couplings.

DOI: 10.1103/PhysRevD.83.114045 PACS numbers: 14.65.Ha, 12.38.Qk, 12.60.−i

I. INTRODUCTION

The Large Hadron Collider (LHC) has started to operate and is already giving us new data [1]. Thereby we will soon be able to explore physics beyond the standard model of the strong and electroweak interactions in TeV world with high precision. Studies of such new physics can be classified into two categories: model-dependent and model-independent approaches. The former approach could enable precise calculations but require us to start everything from the beginning if the wrong model was chosen. In contrast to it, we would rarely fail to get meaningful information in the latter, but it would not be that easy there to perform precision analyses, since we usually need to treat many unknown parameters together.

One reasonable way to decrease the number of such unknown parameters in a model-independent analysis is to assume a new physics characterized by an energy scale Λ and write down $SU(3) \times SU(2) \times U(1)$-symmetric effective operators for the world below Λ. Those operators with dimension 6, having the leading importance, were listed in [2], supposing there exist only standard particles below Λ. Although we still have to treat several operators (parameters) even in this framework, some of the operators given there were found to be dependent on each other through equations of motion [3]. This shows that we might further be able to reduce the number of independent operators, and indeed it was done in [4] (see also [5]).

In this effective-operator framework, not only electroweak couplings but also QCD couplings receive nonstandard corrections. Although it might be hard to imagine that the QCD couplings of light quarks are affected by those anomalous interactions, the top-quark couplings could however be exceptional, because this quark has not been studied enough precisely yet, and its extremely heavy mass seems to tell us something about a new physics beyond the standard model. That is, this heaviest quark might be able to work as a precious window to a nonstandard physics once LHC starts to give us fruitful data.

Under this consideration, we have performed analyses of anomalous top-gluon couplings produced by the dimension-6 operators through $t\bar{t}$ productions at Tevatron and LHC [6,7]. In this article, we would like to develop them and perform more realistic analyses focusing on momentum distributions of the charged lepton coming from the semileptonic top decay in $p\bar{p}/pp \to t\bar{t}X$. In fact, a number of authors have studied top anomalous interactions through such final leptons in $p\bar{p}/pp$ collisions [8–16]. Their main interests are in CP-violation, which is reasonable since the standard-model CP-violation in the top sector is expected so small that any non-negligible CP-violation effects there will be a signal of new physics.

Here, however, we have no mind to add similar studies to them. Our main purpose of revisiting this issue is to present analytical formulas of the final-lepton momentum distributions for practical use, and carry out some computations and analyses based on them, taking into account both anomalous CP-conserving *and* CP-violating top-gluon couplings *plus* nonstandard tbW coupling altogether.

We first describe our calculational framework in Sec. II. In Sec. III, we derive the final-lepton momentum distribution in partonic processes $q\bar{q}/gg \to t\bar{t} \to \ell^+ X$, and present their analytical expressions. We then transform them into the angular, energy and transverse-momentum distributions of the final charged lepton in the hadronic processes $p\bar{p}/pp \to t\bar{t}X \to \ell^+ X'$, and study those distributions numerically for several typical parameter sets in Sec. IV. Finally, a summary and some remarks are given in Sec. V. In the Appendix, we refine our last result on the anomalous top-gluon couplings [7] with the Tevatron and CMS data [17,18] by adding the latest ATLAS data [19].

*hioki@ias.tokushima-u.ac.jp
†ohkuma@fukui-ut.ac.jp

II. FRAMEWORK

Let us describe our basic framework in this section. In Ref. [2] were given three effective operators contributing to top-gluon interactions. Those operators produce top-pair production amplitudes which include γ^μ, $\sigma^{\mu\nu}q_\nu$, $(p_i + p_j)^\mu$, and q^μ terms (or more complicated Lorentz structure), where $p_{i,j}$ and q are the top-quark i, j, and gluon momenta. However, two of them were shown not to be independent in [4], and we only need to take into account one operator

$$\mathcal{O}^{33}_{uG\phi} = \sum_a [\bar{q}_{L3}(x)\lambda^a\sigma^{\mu\nu}u_{R3}(x)\tilde{\phi}(x)G^a_{\mu\nu}(x)], \quad (1)$$

where we followed the notation of [4]: q_{L3} is the third generation of left-handed $SU(2)$-doublet, i.e., $(t, b)^t_L$, u_{R3} is the third generation up-type $SU(2)$ singlet, i.e., t_R, $\tilde{\phi} \equiv i\tau^2\phi^*$ with ϕ being the Higgs doublet, $G^a_{\mu\nu}$ is the $SU(3)$ gauge-field (= gluon) tensor.

Now the top-gluon interaction Lagrangian including the above operator is given by

$$\mathcal{L} = \mathcal{L}_{\rm SM} + \frac{1}{\Lambda^2}(C^{33}_{uG\phi}\mathcal{O}^{33}_{uG\phi} + C^{33*}_{uG\phi}\mathcal{O}^{33\dagger}_{uG\phi}), \quad (2)$$

where $\mathcal{L}_{\rm SM}$ on the right-hand side means the standard-model QCD top-gluon couplings and $C^{33}_{uG\phi}$, the coefficient of $\mathcal{O}^{33}_{uG\phi}$, represents the contribution of this operator. In our framework, this coefficient (plus its complex conjugate) and Λ^{-2} are combined and treated as parameters to be determined by experimental data. Since $\mathcal{O}^{33}_{uG\phi}$ contains $G^a_{\mu\nu}$, the resultant nonstandard interaction has not only $t\bar{t}g$ but also $t\bar{t}gg$ couplings. Let us therefore denote this Lagrangian by $\mathcal{L}_{t\bar{t}g,gg}$ hereafter and reexpress it as

$$\mathcal{L}_{t\bar{t}g,gg} = -\frac{1}{2}g_s\sum_a\Big[\bar{\psi}_t(x)\lambda^a\gamma^\mu\psi_t(x)G^a_\mu(x) - \bar{\psi}_t(x)\lambda^a\frac{\sigma^{\mu\nu}}{m_t}(d_V + id_A\gamma_5)\psi_t(x)G^a_{\mu\nu}(x)\Big], \quad (3)$$

where g_s is the $SU(3)$ coupling constant and $d_{V,A}$ are defined as

$$d_V \equiv \frac{\sqrt{2}vm_t}{g_s\Lambda^2}\,{\rm Re}(C^{33}_{uG\phi}), \qquad d_A \equiv \frac{\sqrt{2}vm_t}{g_s\Lambda^2}\,{\rm Im}(C^{33}_{uG\phi})$$

corresponding to the top chromomagnetic- and chromoelectric-dipole moments, respectively, with v being the Higgs vacuum expectation value (= 246 GeV). Concerning the other light quarks, i.e., u, d, s, c and b, we assume their couplings with the gluon are properly described by the standard QCD Lagrangian, though in principle there also could be nonstandard corrections in our framework, because those couplings have so far been tested very well based on a lot of experimental data.

On the other hand, dimension-6 operators which contribute to top-decay $t \to bW$ are

$$\mathcal{O}^{(3,33)}_{\phi q} = i\sum_I[\phi^\dagger(x)\tau^I D_\mu\phi(x)][\bar{q}_{L3}(x)\gamma^\mu\tau^I q_{L3}(x)] \quad (4)$$

$$\mathcal{O}^{33}_{\phi\phi} = i[\tilde{\phi}^\dagger(x)D_\mu\phi(x)][\bar{u}_{R3}(x)\gamma^\mu d_{R3}(x)] \quad (5)$$

$$\mathcal{O}^{33}_{uW} = \sum_I \bar{q}_{L3}(x)\sigma^{\mu\nu}\tau^I u_{R3}(x)\tilde{\phi}(x)W^I_{\mu\nu}(x) \quad (6)$$

$$\mathcal{O}^{33}_{dW} = \sum_I \bar{q}_{L3}(x)\sigma^{\mu\nu}\tau^I d_{R3}(x)\phi(x)W^I_{\mu\nu}(x), \quad (7)$$

where D_μ is the $SU(2) \times U(1)$ covariant derivative, d_{R3} is the third generation down-type $SU(2)$ singlet (i.e., b_R), and $W^I_{\mu\nu}$ is the $SU(2)$ gauge-field tensor.

We thereby have the corresponding interaction Lagrangian

$$\mathcal{L} = \mathcal{L}_{\rm SM} + \frac{1}{\Lambda^2}\sum_i(C_i\mathcal{O}_i + C^*_i\mathcal{O}^\dagger_i), \quad (8)$$

where $\mathcal{L}_{\rm SM}$ gives the standard-model tbW couplings this time and the sum is taken over the above four operators. We denote this Lagrangian by $\mathcal{L}_{tbW}$ and again reexpress as

$$\mathcal{L}_{tbW} = -\frac{g}{\sqrt{2}}\Big[\bar{\psi}_b(x)\gamma^\mu(f^L_1P_L + f^R_1P_R)\psi_t(x)W^-_\mu(x) + \bar{\psi}_b(x)\frac{\sigma^{\mu\nu}}{M_W}(f^L_2P_L + f^R_2P_R)\psi_t(x)\partial_\mu W^-_\nu(x)\Big], \quad (9)$$

where g is the $SU(2)$ coupling constant, $P_{L/R} \equiv (1 \mp \gamma_5)/2$,

$$f^L_1 \equiv V_{tb} + C^{(3,33)*}_{\phi q}\frac{v^2}{\Lambda^2}, \qquad f^R_1 \equiv C^{33*}_{\phi\phi}\frac{v^2}{2\Lambda^2},$$
$$f^L_2 \equiv -\sqrt{2}C^{33*}_{dW}\frac{v^2}{\Lambda^2}, \qquad f^R_2 \equiv -\sqrt{2}C^{33}_{uW}\frac{v^2}{\Lambda^2}$$

and V_{tb} is (tb) element of Kobayashi-Maskawa matrix. Here again $\ell\nu W$ couplings, which become necessary for $W^+ \to \ell^+\nu_\ell$ occurring after $t \to bW^+$, could also have nonstandard terms, but we adopt the SM Lagrangian for this part due to the same reason as the light-quark and gluon interactions.

In calculating the momentum distributions of the final charged lepton in the partonic level, we utilize the Kawasaki-Shirafuji-Tsai formalism [20,21]. This formalism is quite valuable when we study the momentum distribution of a final-state particle from productions/decays of a

heavy particle whose mass m and total width Γ satisfy $m \gg \Gamma$, and consequently "narrow-width approximation"

$$\left| \frac{1}{p^2 - m^2 + im\Gamma} \right|^2 \simeq \frac{\pi}{m\Gamma} \delta(p^2 - m^2)$$

holds as a good approximation. In this framework, the final-lepton momentum distribution in a collision of particles a and b like $ab \to t\bar{t} \to \ell^+ X$ is given by

$$\frac{d\sigma}{d^3\boldsymbol{p}_\ell}(ab \to t\bar{t} \to \ell^+ X) = 4 \int d\Omega_t \frac{d\sigma}{d\Omega_t}(n, 0) \times \frac{1}{\Gamma_t} \frac{d\Gamma_\ell}{d^3\boldsymbol{p}_\ell}(t \to b\ell^+ \nu), \quad (10)$$

where Γ_ℓ is the width of an unpolarized top, $d\sigma(n, 0)/d\Omega_t$ is that obtained from the $t\bar{t}$-production cross section with spin vectors s_t and $s_{\bar{t}}$, $d\sigma(s_t, s_{\bar{t}})/d\Omega_t$, through the following replacement:

$$s_t^\mu \to n^\mu = \frac{m_t}{p_t p_\ell} p_\ell^\mu - \frac{1}{m_t} p_t^\mu, \qquad s_{\bar{t}}^\mu \to 0. \quad (11)$$

We get the ℓ^- distribution from $\bar{t}$ decay by exchanging the roles of s_t and $s_{\bar{t}}$, and reversing the sign of n.

III. PARTON-PROCESS CROSS SECTIONS

Let us derive the lepton-momentum distribution in the parton processes $q\bar{q}/gg \to t\bar{t} \to \ell^+ X$ using interactions (3) and (9) in Kawasaki-Shirafuji-Tsai framework. In [22] is pointed out that we have to be careful in applying the narrow-width approximation to a certain process, but in the case of the top quark and W boson, necessary conditions are satisfied as $m_t (= 172.0 \pm 1.6\,\text{GeV}) \gg \Gamma_t (= 1.99^{+0.69}_{-0.55}\,\text{GeV})$ and $M_W (= 80.399 \pm 0.023\,\text{GeV}) \gg \Gamma_W (= 2.085 \pm 0.042\,\text{GeV})$ [23,24].

In the following calculations, we neglect all the fermion masses except the top, and put V_{tb} to be 1 [25]. In addition, we take into account all the contributions from $d_{V,A}$ since this is part of the strong interaction, although LHC data have narrowed the allowed region for them [7], while we include only linear terms in anomalous $f_{1,2}^{L,R}$ like in [13] considering that this is electroweak interaction and also that all Tevatron data on $t \to bW$ [26,27] are consistent with the standard model (i.e., $f_1^L = 1$, $f_1^R = f_2^{L,R} = 0$).

Under these approximations, the $q\bar{q}/gg \to t\bar{t}$ differential cross sections are

$$\frac{d\sigma_{q\bar{q}}}{d\Omega_t}(s_t, 0) = \frac{\hat{\beta}\alpha_s^2}{36\hat{s}}[1 - 2(v - z) - 8(d_V - d_V^2 + d_A^2) + 8(d_V^2 + d_A^2)v/z] \quad (12)$$

$$\frac{d\sigma_{gg}}{d\Omega_t}(s_t, 0) = \frac{\hat{\beta}\alpha_s^2}{384\hat{s}}[(4/v - 9)[1 - 2v + 4z(1 - z/v) - 8d_V(1 - 2d_V)] + 4(d_V^2 + d_A^2)[14(1 - 4d_V)/z + (1 + 10d_V)/v] - 32(d_V^2 + d_A^2)^2(1/z - 1/v - 4v/z^2)] \quad (13)$$

in the CM frame, and the $t \to bW \to b\ell^+\nu$ differential width is

$$\frac{1}{\Gamma_t}\frac{d\Gamma_\ell}{d^3\boldsymbol{p}_\ell} = \frac{6B_\ell}{\pi m_t^2 W E_\ell} \omega \left[1 + 2d_R\left(\frac{1}{1 - \omega} - \frac{3}{1 + 2r}\right)\right], \quad (14)$$

where E_ℓ is the ℓ^+ energy, i.e., $p_\ell^\mu = (E_\ell, \boldsymbol{p}_\ell)$,

$$z \equiv m_t^2/\hat{s}, \qquad v \equiv (\hat{t} - m_t^2)(\hat{u} - m_t^2)/\hat{s}^2,$$
$$\omega \equiv (p_t - p_\ell)^2/m_t^2, \qquad r \equiv (M_W/m_t)^2,$$
$$W \equiv (1 - r)^2(1 + 2r), \qquad d_R \equiv \text{Re}(f_2^R)\sqrt{r},$$

$\hat{s}$, $\hat{t}$, $\hat{u}$ are the Mandelstam variables, $\hat{\beta} \equiv \sqrt{1 - 4m_t^2/\hat{s}}$ is the size of the top velocity, B_ℓ is the top-semileptonic-decay branching ratio ($= \Gamma_\ell/\Gamma_t$), and we applied the narrow-width approximation to the W propagator. Here we attached "$\hat{}$" to some variables to clarify that they are parton-level ones. Note that neither $d\sigma_{q\bar{q}}$ nor $d\sigma_{gg}$ has s_t-dependent terms actually.

Combining all those formulas and quantities with Eq. (10) we arrive at the lepton-momentum distributions:

$$\frac{d\sigma_{ab}}{dE_\ell dc_\ell} = \left[\frac{d\sigma_{ab}}{dE_\ell dc_\ell}\right]_{\text{SM}} + \left[\frac{d\Delta\sigma_{ab}}{dE_\ell dc_\ell}\right]_{\text{BSM}} \quad (15)$$

where $ab = q\bar{q}$ or gg, the first (SM)/second (BSM) terms on the right-hand side express, respectively, the standard-model/beyond-the-standard-model contributions, and c_ℓ is our abbreviation of $\cos\theta_\ell$ with θ_ℓ being the scattering angle between the momenta of the incident parton a and ℓ^+ (similarly $s_\ell \equiv \sin\theta_\ell$ hereafter). We give their analytical forms explicitly in the following:

$$\left[\frac{d\sigma_{q\bar{q}}}{dE_\ell dc_\ell}\right]_{\text{SM}} = \frac{4\hat{\beta}\alpha_s^2}{3m_t^2\hat{s}} \frac{B_\ell}{W} E_\ell[(1 + 2z)\mathcal{F}_0(E_\ell, c_\ell) - 2\mathcal{F}_1(E_\ell, c_\ell)] \quad (16)$$

$$\left[\frac{d\Delta\sigma_{q\bar{q}}}{dE_\ell dc_\ell}\right]_{\rm BSM} = \frac{4\hat{\beta}\alpha_s^2}{3m_t^2\hat{s}}\frac{B_\ell}{W}E_\ell\Big[2d_R\Big[(1+2z)\Big(\mathcal{G}_0(E_\ell,c_\ell)-\frac{3}{1+2r}\mathcal{F}_0(E_\ell,c_\ell)\Big)-2\Big(\mathcal{G}_1(E_\ell,c_\ell)-\frac{3}{1+2r}\mathcal{F}_1(E_\ell,c_\ell)\Big)\Big]$$
$$-8(d_V-d_V^2+d_A^2)\mathcal{F}_0(E_\ell,c_\ell)+\frac{8}{z}(d_V^2+d_A^2)\mathcal{F}_1(E_\ell,c_\ell)-16d_R(d_V-d_V^2+d_A^2)$$
$$\times\Big(\mathcal{G}_0(E_\ell,c_\ell)-\frac{3}{1+2r}\mathcal{F}_0(E_\ell,c_\ell)\Big)+\frac{16}{z}d_R(d_V^2+d_A^2)\Big(\mathcal{G}_1(E_\ell,c_\ell)-\frac{3}{1+2r}\mathcal{F}_1(E_\ell,c_\ell)\Big)\Big] \quad (17)$$

$$\left[\frac{d\sigma_{gg}}{dE_\ell dc_\ell}\right]_{\rm SM} = \frac{\hat{\beta}\alpha_s^2}{8m_t^2\hat{s}}\frac{B_\ell}{W}E_\ell[-(17+36z)\mathcal{F}_0(E_\ell,c_\ell)+18\mathcal{F}_1(E_\ell,c_\ell)+4(1+4z+9z^2)\mathcal{F}_{-1}(E_\ell,c_\ell)-16z^2\mathcal{F}_{-2}(E_\ell,c_\ell)] \quad (18)$$

$$\left[\frac{d\Delta\sigma_{gg}}{dE_\ell dc_\ell}\right]_{\rm BSM} = \frac{\hat{\beta}\alpha_s^2}{8m_t^2\hat{s}}\frac{B_\ell}{W}E_\ell\Big[2d_R\Big[-(17+36z)\Big(\mathcal{G}_0(E_\ell,c_\ell)-\frac{3}{1+2r}\mathcal{F}_0(E_\ell,c_\ell)\Big)$$
$$+18\Big(\mathcal{G}_1(E_\ell,c_\ell)-\frac{3}{1+2r}\mathcal{F}_1(E_\ell,c_\ell)\Big)+4(1+4z+9z^2)\Big(\mathcal{G}_{-1}(E_\ell,c_\ell)-\frac{3}{1+2r}\mathcal{F}_{-1}(E_\ell,c_\ell)\Big)$$
$$-16z^2\Big(\mathcal{G}_{-2}(E_\ell,c_\ell)-\frac{3}{1+2r}\mathcal{F}_{-2}(E_\ell,c_\ell)\Big)\Big]-8d_V(1-2d_V)(4\mathcal{F}_{-1}(E_\ell,c_\ell)-9\mathcal{F}_0(E_\ell,c_\ell))$$
$$+4(d_V^2+d_A^2)\Big(\frac{14}{z}(1-4d_V)\mathcal{F}_0(E_\ell,c_\ell)+(1+10d_V)\mathcal{F}_{-1}(E_\ell,c_\ell)\Big)-32(d_V^2+d_A^2)^2$$
$$\times\Big(\frac{1}{z}\mathcal{F}_0(E_\ell,c_\ell)-\mathcal{F}_{-1}(E_\ell,c_\ell)-\frac{4}{z^2}\mathcal{F}_1(E_\ell,c_\ell)\Big)-16d_Rd_V(1-2d_V)\Big[4\Big(\mathcal{G}_{-1}(E_\ell,c_\ell)-\frac{3}{1+2r}\mathcal{F}_{-1}(E_\ell,c_\ell)\Big)$$
$$-9\Big(\mathcal{G}_0(E_\ell,c_\ell)-\frac{3}{1+2r}\mathcal{F}_0(E_\ell,c_\ell)\Big)\Big]+8d_R(d_V^2+d_A^2)\Big[\frac{14}{z}(1-4d_V)\Big(\mathcal{G}_0(E_\ell,c_\ell)-\frac{3}{1+2r}\mathcal{F}_0(E_\ell,c_\ell)\Big)$$
$$+(1+10d_V)\Big(\mathcal{G}_{-1}(E_\ell,c_\ell)-\frac{3}{1+2r}\mathcal{F}_{-1}(E_\ell,c_\ell)\Big)\Big]-64d_R(d_V^2+d_A^2)^2\Big[\frac{1}{z}\Big(\mathcal{G}_0(E_\ell,c_\ell)-\frac{3}{1+2r}\mathcal{F}_0(E_\ell,c_\ell)\Big)$$
$$-\mathcal{G}_{-1}(E_\ell,c_\ell)+\frac{3}{1+2r}\mathcal{F}_{-1}(E_\ell,c_\ell)-\frac{4}{z^2}\Big(\mathcal{G}_1(E_\ell,c_\ell)-\frac{3}{1+2r}\mathcal{F}_1(E_\ell,c_\ell)\Big)\Big]\Big]. \quad (19)$$

Here $\mathcal{F}_m$ and $\mathcal{G}_m(m=-2,-1,0,+1)$ are Ω_t integrations choosing the $\boldsymbol{p}_\ell$ direction as the z axis

$$\mathcal{F}_m(E_\ell,c_\ell)\equiv\int_{c_{t-}}^{c_{t+}}dc_t\int_0^{2\pi}d\phi_t\omega v^m$$
$$\mathcal{G}_m(E_\ell,c_\ell)\equiv\int_{c_{t-}}^{c_{t+}}dc_t\int_0^{2\pi}d\phi_t\frac{\omega}{1-\omega}v^m$$

($c_t\equiv\cos\theta_t$) with

$$c_{t+}=\mathrm{Max}\Big[\mathrm{Min}\Big[\frac{1}{\hat{\beta}}\Big(1-\frac{M_W^2}{\sqrt{\hat{s}}E_\ell}\Big),+1\Big],-1\Big]$$
$$c_{t-}=\mathrm{Min}\Big[\mathrm{Max}\Big[\frac{1}{\hat{\beta}}\Big(1-\frac{m_t^2}{\sqrt{\hat{s}}E_\ell}\Big),-1\Big],+1\Big] \quad (20)$$

(see also [28]), and they are given as

$$\mathcal{F}_m=I_m(c_{t+})-I_m(c_{t-}),\qquad \mathcal{G}_m=J_m(c_{t+})-J_m(c_{t-}), \quad (21)$$

where each I_m and J_m are

$$I_1(c_t)=-\frac{\pi}{4(1-\hat{\beta})}c_t\Big[(1-\hat{\beta}-x_\ell)\times\Big(\hat{\beta}^2s_\ell^2-2+\frac{1}{3}\hat{\beta}^2(3c_\ell^2-1)c_t^2\Big)+\frac{1}{4}\hat{\beta}x_\ell[2(\hat{\beta}^2s_\ell^2-2)c_t+\hat{\beta}^2(3c_\ell^2-1)c_t^3]\Big] \quad (22)$$

$$I_0(c_t)=\frac{\pi}{1-\hat{\beta}}c_t[2(1-\hat{\beta}-x_\ell)+\hat{\beta}x_\ell c_t] \quad (23)$$

$$I_{-1}(c_t)=\frac{4\pi}{1-\hat{\beta}}[(1-\hat{\beta}-x_\ell)[f_{0/1}^+(c_t)+f_{0/1}^-(c_t)]+\hat{\beta}x_\ell[f_{1/1}^+(c_t)+f_{1/1}^-(c_t)]] \quad (24)$$

$$I_{-2}(c_t)=\frac{8\pi}{1-\hat{\beta}}[(1-\hat{\beta}-x_\ell)[\hat{\beta}c_\ell f_{1/3}^+(c_t)+f_{0/3}^+(c_t)-\hat{\beta}c_\ell f_{1/3}^-(c_t)+f_{0/3}^-(c_t)+f_{0/1}^+(c_t)+f_{0/1}^-(c_t)]+\hat{\beta}x_\ell[\hat{\beta}c_\ell f_{2/3}^+(c_t)+f_{1/3}^+(c_t)-\hat{\beta}c_\ell f_{2/3}^-(c_t)+f_{1/3}^-(c_t)+f_{1/1}^+(c_t)+f_{1/1}^-(c_t)]] \quad (25)$$

$$J_1(c_t) = \frac{\pi}{4}\Big[\frac{1}{\hat{\beta}x_\ell}(1-\hat{\beta})(\hat{\beta}^2-3)s_\ell^2\ln(1-\hat{\beta}c_t) + \frac{1}{2x_\ell}(1-\hat{\beta})(3c_\ell^2-1)c_t(2+\hat{\beta}c_t) + (\hat{\beta}^2 s_\ell^2-2)c_t + \frac{1}{3}\hat{\beta}^2(3c_\ell^2-1)c_t^3\Big] \quad (26)$$

$$J_0(c_t) = -\frac{2\pi}{\hat{\beta}}\Big[\frac{1-\hat{\beta}}{x_\ell}\ln(1-\hat{\beta}c_t) + \hat{\beta}c_t\Big] \quad (27)$$

$$J_{-1}(c_t) = 4\pi\Big[\frac{1-\hat{\beta}}{x_\ell}[g^+_{0/1}(c_t) + g^-_{0/1}(c_t)] - f^+_{0/1}(c_t) - f^-_{0/1}(c_t)\Big] \quad (28)$$

$$J_{-2}(c_t) = 8\pi\Big[\frac{1-\hat{\beta}}{x_\ell}[\hat{\beta}c_\ell g^+_{1/3}(c_t) + g^+_{0/3}(c_t) - \hat{\beta}c_\ell g^-_{1/3}(c_t) + g^-_{0/3}(c_t) + g^+_{0/1}(c_t) + g^-_{0/1}(c_t)] - \hat{\beta}c_\ell f^+_{1/3}(c_t) - f^+_{0/3}(c_t) + \hat{\beta}c_\ell f^-_{1/3}(c_t) - f^-_{0/3}(c_t) - f^+_{0/1}(c_t) - f^-_{0/1}(c_t)\Big] \quad (29)$$

with $x_\ell \equiv 2E_\ell\sqrt{(1-\hat{\beta})/(1+\hat{\beta})}/m_t$, and $f^\pm_{m/n}$ and $g^\pm_{m/n}$ being

$$f^\pm_{m/n}(c_t) \equiv \int dc_t \frac{c_t^m}{\sqrt{(\hat{\beta}^2c_t^2 \pm 2\hat{\beta}c_\ell c_t + 1 - \hat{\beta}^2 s_\ell^2)^n}} \quad (30)$$

$$g^\pm_{m/n}(c_t) \equiv \int dc_t \frac{c_t^m}{(1-\hat{\beta}c_t)\sqrt{(\hat{\beta}^2c_t^2 \pm 2\hat{\beta}c_\ell c_t + 1 - \hat{\beta}^2 s_\ell^2)^n}}. \quad (31)$$

Their explicit forms after the integrations are

$$f^\pm_{0/1}(c_t) = \frac{1}{\hat{\beta}}\ln[\hat{\beta}c_t \pm c_\ell + R_\pm(c_t)] \quad (32)$$

$$f^\pm_{1/1}(c_t) = \frac{1}{\hat{\beta}^2}[R_\pm \mp c_\ell \ln[\hat{\beta}c_t \pm c_\ell + R_\pm(c_t)]] \quad (33)$$

$$f^\pm_{0/3}(c_t) = \frac{\hat{\beta}c_t \pm c_\ell}{\hat{\beta}(1-\hat{\beta}^2)s_\ell^2 R_\pm(c_t)} \quad (34)$$

$$f^\pm_{1/3}(c_t) = -\frac{1-\hat{\beta}^2 s_\ell^2 \pm \hat{\beta}c_\ell c_t}{\hat{\beta}^2(1-\hat{\beta}^2)s_\ell^2 R_\pm(c_t)} \quad (35)$$

$$f^\pm_{2/3}(c_t) = \frac{1}{\hat{\beta}^3}\Big[\frac{\hat{\beta}(2c_\ell^2 - 1 + \hat{\beta}^2 s_\ell^2)c_t \pm c_\ell(1-\hat{\beta}^2 s_\ell^2)}{(1-\hat{\beta}^2)s_\ell^2 R_\pm(c_t)} + \ln[\hat{\beta}c_t \pm c_\ell + R_\pm(c_t)]\Big] \quad (36)$$

$$g^\pm_{0/1}(c_t) = -\frac{1}{\hat{\beta}Q_\pm}\ln\Big[\frac{1-\hat{\beta}c_t}{(1\pm c_\ell)(1-\hat{\beta}^2 \pm \hat{\beta}^2 c_\ell + \hat{\beta}c_t) + Q_\pm R_\pm(c_t)}\Big] \quad (37)$$

$$g^\pm_{0/3}(c_t) = -\frac{1 \mp 2c_\ell - \hat{\beta}^2(1\mp c_\ell) - \hat{\beta}c_t}{\hat{\beta}s_\ell^2[2-\hat{\beta}^2(3\mp c_\ell) + \hat{\beta}^4(1\mp c_\ell)]R_\pm(c_t)} - \frac{1}{\hat{\beta}Q_\pm^3}\ln\Big[\frac{1-\hat{\beta}c_t}{(1\pm c_\ell)(1-\hat{\beta}^2 \pm \hat{\beta}^2 c_\ell + \hat{\beta}c_t) + Q_\pm R_\pm(c_t)}\Big] \quad (38)$$

$$g^\pm_{1/3}(c_t) = \frac{1}{\hat{\beta}}[g^\pm_{0/3}(c_t) - f^\pm_{0/3}(c_t)], \quad (39)$$

where

$$R_\pm(c_t) \equiv \sqrt{\hat{\beta}^2c_t^2 \pm 2\hat{\beta}c_\ell c_t + 1 - \hat{\beta}^2 s_\ell^2},$$
$$Q_\pm \equiv \sqrt{2 \pm 2c_\ell - \hat{\beta}^2 s_\ell^2}$$

and all terms which cancel out in $f^\pm_{m/n}(c_{t+}) - f^\pm_{m/n}(c_{t-})$ and $g^\pm_{m/n}(c_{t+}) - g^\pm_{m/n}(c_{t-})$ have been dropped from the beginning, although the right-hand sides of Eqs. (30) and (31), the definition of $f^\pm_{m/n}$ and $g^\pm_{m/n}$, mean indefinite integrals.

IV. FINAL-LEPTON DISTRIBUTIONS

We are now in the final stage of computing the lepton-momentum distributions under actual experimental conditions. In order to derive hadron cross sections based on the parton-level formulas given in the previous section, we first need to connect partonic cross sections in the parton-CM frame and hadron-CM frame. The final-lepton energy and scattering angle in the parton-CM frame, E^*_ℓ and θ^*_ℓ, are expressed in terms of those in the hadron-CM frame, E_ℓ and θ_ℓ, as

$$E_\ell^* = E_\ell(1-\beta_{\rm L}c_\ell)/\sqrt{1-\beta_{\rm L}^2},$$
$$c_\ell^* = (c_\ell-\beta_{\rm L})/(1-\beta_{\rm L}c_\ell), \tag{40}$$

where $\beta_{\rm L}$ is the Lorentz-transformation boost factor connecting the two frames. These relations lead to Jacobian

$$\partial(E_\ell^*, c_\ell^*)/\partial(E_\ell, c_\ell) = E_\ell/E_\ell^* \tag{41}$$

and consequently cross-section relation

$$\frac{d\sigma_{q\bar{q},gg}}{dE_\ell dc_\ell} = \frac{E_\ell}{E_\ell^*}\frac{d\sigma_{q\bar{q},gg}}{dE_\ell^* dc_\ell^*}. \tag{42}$$

Then the hadron cross sections are obtained by integrating the product of *the parton-distribution functions* and *the parton cross sections in the hadron-CM frame* on the momentum fractions x_1 and x_2 carried by the partons:

$$\frac{d\sigma_{p\bar{p}/pp}}{dE_\ell dc_\ell} = \sum_{a,b}\int_{4m_t^2/s}^1 dx_1 \int_{4m_t^2/(x_1 s)}^1 dx_2 N_a(x_1)N_b(x_2) \times \frac{E_\ell}{E_\ell^*}\frac{d\sigma_{ab}}{dE_\ell^* dc_\ell^*}, \tag{43}$$

where $N_{a,b}(x)$ are the parton-distribution functions of parton a and b ($a, b = u, \bar{u}, d, \bar{d}, s, \bar{s}, c, \bar{c}, b, \bar{b}$ or g) and the boost factor is given by $\beta_{\rm L} = (x_1 - x_2)/(x_1 + x_2)$. Note here that s is defined via the initial hadron momenta $p_{p/\bar{p}}$ as $s \equiv (p_p + p_{p/\bar{p}})^2$.

A. Angular distribution

We first study the angular distribution:

$$\frac{d\sigma_{p\bar{p}/pp}}{dc_\ell} = \int_{E_\ell^-}^{E_\ell^+} dE_\ell \frac{d\sigma_{p\bar{p}/pp}}{dE_\ell dc_\ell}, \tag{44}$$

where

$$E_\ell^+ = \frac{m_t^2}{\sqrt{s}(1-\beta)}, \qquad E_\ell^- = \frac{M_W^2}{\sqrt{s}(1+\beta)}$$

and $\beta \equiv \sqrt{1-4m_t^2/s}$. Concerning the anomalous-coupling parameters, we take

$$(d_V, d_A) = {\rm (a)}(-0.01, 0), \quad {\rm (b)}(0.01, 0), \quad {\rm (c)}(0, 0.05), \quad {\rm (d)}(0.03, 0.10)$$

as typical examples,[1] and we use $\alpha_s = 0.118$, $M_W = 80.4$ GeV, $B_\ell = 0.22(\ell = e/\mu)$, and the present world average $m_t = 172$ GeV [29]. Note that the decay anomalous parameter d_R does not contribute to the angular distribution due to the decoupling theorem [30–32]. As for the parton-distribution functions, we adopt the latest set "CTEQ6.6M" in next-to-next-to-leading-order (NNLO) approximation [33].

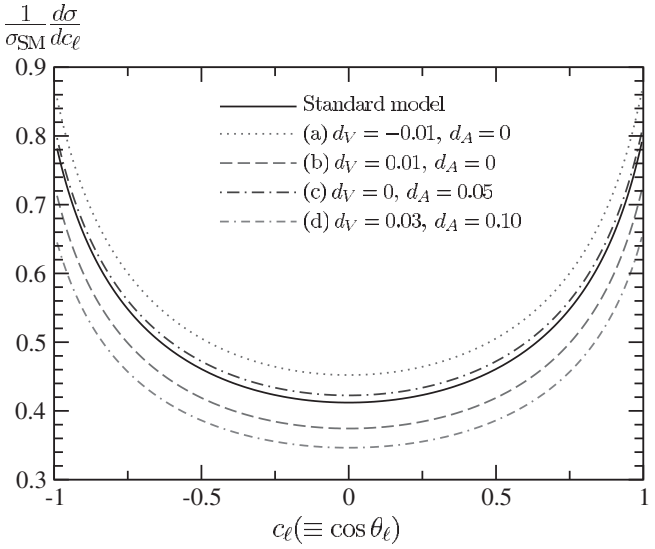

FIG. 1. The final-lepton angular distribution normalized by $\sigma_{\rm SM}$: Tevatron energy $\sqrt{s} = 1.96$ TeV.

We present the results in Figs. 1–3 for Tevatron, LHC (7 TeV) and LHC(14 TeV), respectively, where we show the distributions normalized by the standard-model total cross section $\sigma_{\rm SM} \equiv \sigma(p\bar{p}/pp \to t\bar{t}X \to \ell^+ X') = B_\ell \sigma(p\bar{p}/pp \to t\bar{t}X)$ so that large part of the QCD corrections cancel each other in the ratio.[2] It should be noted that the vertical axis of Fig. 1 is different from those of Figs. 2 and 3 in scale.

Through those figures, we find that the deviation from $d\sigma_{\rm SM}$ varies to a certain extent to positive or negative direction depending on the anomalous parameters, even if we strictly take into account the constraints on $d_{V,A}$ coming from combined Tevatron and LHC data shown in the Appendix and change parameter values only within the resultant allowed region. In some cases, it will not be easy to distinguish the curves: In particular, those with parameter sets (a) and (c) almost overlap each other in Figs. 2 and 3.

In order to clarify the size of those nonstandard effects more quantitatively, let us show

$$\delta(*) \equiv [d\sigma(*) - d\sigma_{\rm SM}]/d\sigma_{\rm SM}(\times 100)$$

at $\cos\theta_\ell = 0$ as an example, where $*$ means parameter set (a), (b), (c) or (d):

Tevatron

$$\delta({\rm a}) = +9.73\%, \qquad \delta({\rm b}) = -9.15\%,$$
$$\delta({\rm c}) = +2.54\%, \qquad \delta({\rm d}) = -15.94\%. \tag{45}$$

[1] As you find in the Appendix, these values are not excluded by the current experimental data (see Fig. 10). From now on, we only use such values as typical parameter sets.

[2] Strictly speaking, of course, the QCD corrections to the total cross sections and differential cross sections are not the same as each other, but the difference is not that sizable as studied systematically in [34] (see also [35]).

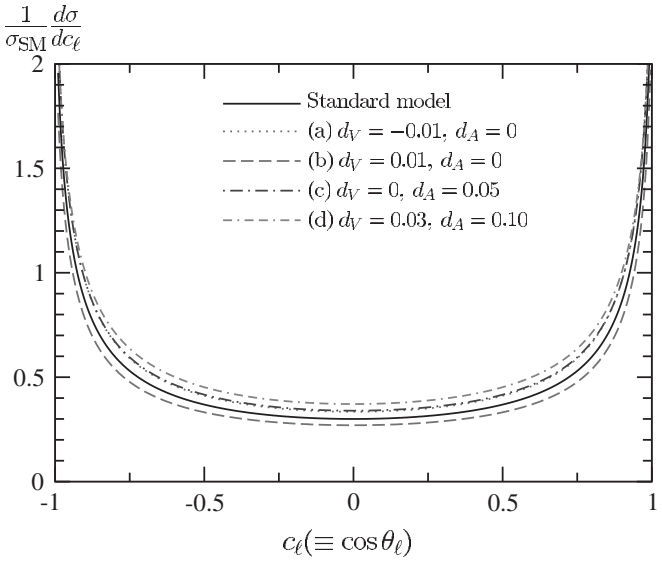

FIG. 2. The final-lepton angular distribution normalized by σ_{SM}: LHC energy $\sqrt{s} = 7$ TeV.

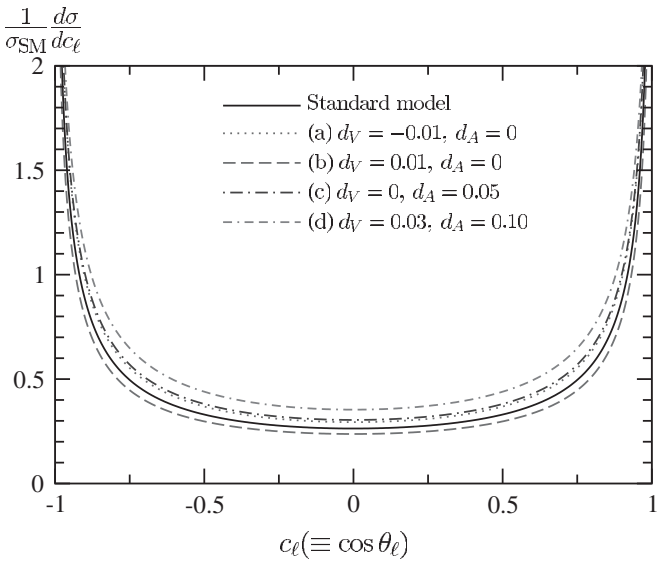

FIG. 3. The final-lepton angular distribution normalized by σ_{SM}: LHC energy $\sqrt{s} = 14$ TeV.

LHC (7 TeV)

$$\delta(\mathrm{a}) = +11.50\%, \qquad \delta(\mathrm{b}) = -10.02\%,$$
$$\delta(\mathrm{c}) = +13.20\%, \qquad \delta(\mathrm{d}) = +23.82\%. \tag{46}$$

LHC (14 TeV)

$$\delta(\mathrm{a}) = +11.61\%, \qquad \delta(\mathrm{b}) = -9.95\%,$$
$$\delta(\mathrm{c}) = +15.60\%, \qquad \delta(\mathrm{d}) = +34.31\%. \tag{47}$$

The deviation could be as large as more than 30% at LHC, and there seem to be some chances of getting a nonstandard signal.

B. Energy distribution

Let us next study the energy distribution:

$$\frac{d\sigma_{p\bar{p}/pp}}{dE_\ell} = \int_{c_\ell^-}^{c_\ell^+} dc_\ell \frac{d\sigma_{p\bar{p}/pp}}{dE_\ell dc_\ell}, \tag{48}$$

where

$$c_\ell^+ = +1, \qquad c_\ell^- = -1.$$

In the same way as the angular distributions, we show the normalized distributions in Figs. 4–6 using anomalous-coupling parameters:

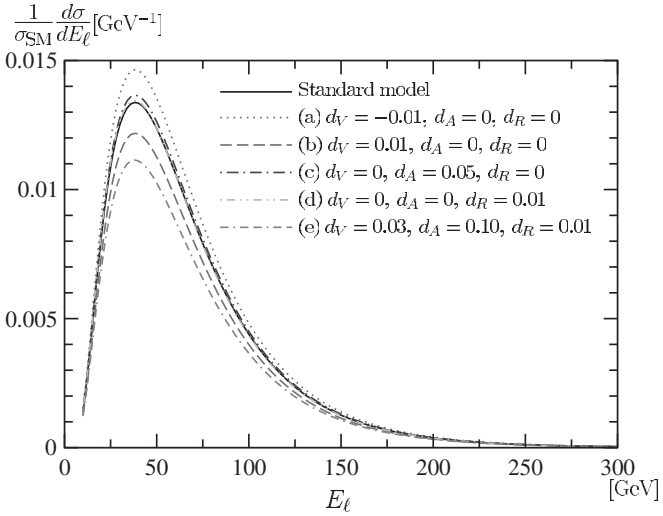

FIG. 4. The final-lepton energy distribution normalized by σ_{SM}: Tevatron energy $\sqrt{s} = 1.96$ TeV.

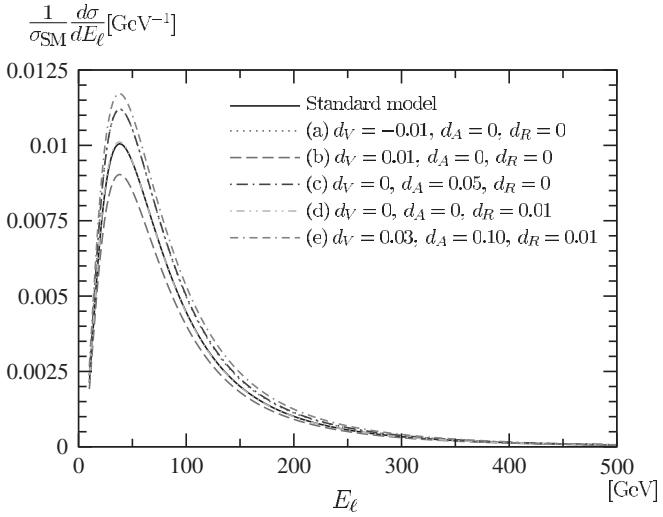

FIG. 5. The final-lepton energy distribution normalized by σ_{SM}: LHC energy $\sqrt{s} = 7$ TeV.

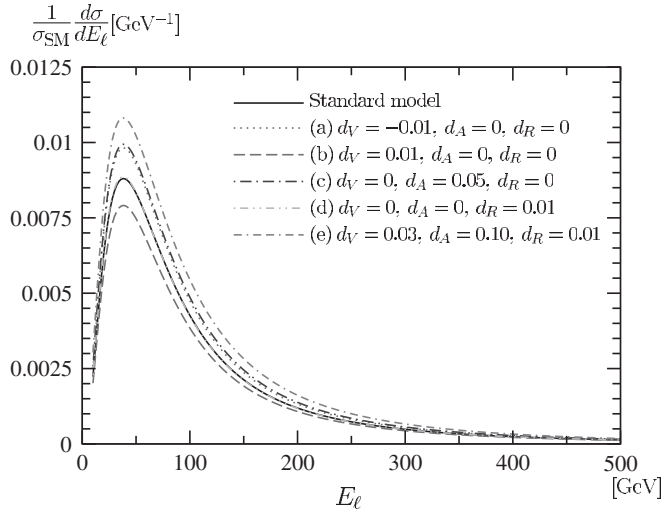

FIG. 6. The final-lepton energy distribution normalized by σ_{SM}: LHC energy $\sqrt{s} = 14$ TeV.

$$(d_V, d_A, d_R) = \text{(a) } (-0.01, 0, 0), \quad \text{(b) } (0.01, 0, 0),$$
$$\text{(c) } (0, 0.05, 0), \quad \text{(d) } (0, 0, 0.01),$$
$$\text{(e) } (0.03, 0.10, 0.01).$$

Note that the d_R terms can also contribute to the results in this case.

We see that sizable effects can be expected in some cases. However, Figs. 4–6 tell us that the dash-dot-dotted curve depicted with parameter set (d) has a substantial overlap with the SM curve, which indicates that we have little chance to observe any signal in this case. In addition, those with parameter sets (a) and (c) show quite similar behavior at LHC and will be indistinguishable from each other, though the overlapping part gets smaller as the center-of-mass energy increases.

We again show the size of the deviations in percentage at $E_\ell = 50$ GeV:

Tevatron

$$\delta(\text{a}) = +9.48\%, \quad \delta(\text{b}) = -8.94\%,$$
$$\delta(\text{c}) = +2.13\%, \quad \delta(\text{d}) = +0.02\%, \tag{49}$$
$$\delta(\text{e}) = -17.08\%.$$

LHC (7 TeV)

$$\delta(\text{a}) = +11.46\%, \quad \delta(\text{b}) = -10.12\%,$$
$$\delta(\text{c}) = +11.45\%, \quad \delta(\text{d}) = +0.20\%, \tag{50}$$
$$\delta(\text{e}) = +16.42\%.$$

LHC (14 TeV)

$$\delta(\text{a}) = +11.58\%, \quad \delta(\text{b}) = -10.11\%,$$
$$\delta(\text{c}) = +13.02\%, \quad \delta(\text{d}) = +0.25\%, \tag{51}$$
$$\delta(\text{e}) = +22.92\%.$$

The size of the deviation is similar to that of the angular distribution, and it could be fairly large though depending on the parameters.

C. Transverse-momentum distribution

Finally, we compute the transverse-momentum p_T distribution. This distribution is obtained by integrating $d\sigma_{p\bar{p}/pp}/dp_T dc_\ell$ over c_ℓ, which cross section is connected with $d\sigma_{p\bar{p}/pp}/dE_\ell dc_\ell$ through Jacobian $1/\sqrt{1-c_\ell^2}$:

$$\frac{d\sigma_{p\bar{p}/pp}}{dp_T} = \int_{c_\ell^-}^{c_\ell^+} dc_\ell \frac{1}{\sqrt{1-c_\ell^2}} \frac{d\sigma_{p\bar{p}/pp}}{dE_\ell dc_\ell}, \tag{52}$$

where

$$c_\ell^+ = -c_\ell^- = \sqrt{1-(p_T/E_\ell^+)^2}$$

and E_ℓ^+ is given in Eq. (44). Using the same anomalous-coupling parameters as for the energy distributions

$$(d_V, d_A, d_R) = \text{(a) } (-0.01, 0, 0), \quad \text{(b) } (0.01, 0, 0),$$
$$\text{(c) } (0, 0.05, 0), \quad \text{(d) } (0, 0, 0.01),$$
$$\text{(e) } (0.03, 0.10, 0.01),$$

the distributions are shown in Figs. 7–9.

In these figures, the shapes of the curves are similar to those in Figs. 4–6. However, the magnitude of these p_T distributions is roughly 2 times larger than that of the E_ℓ

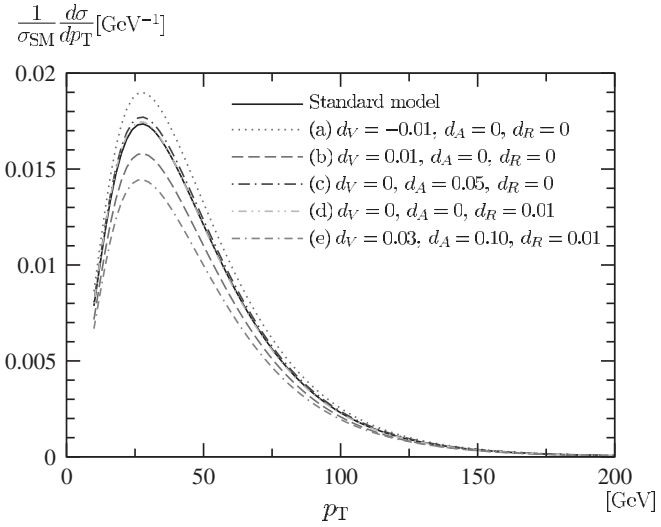

FIG. 7. The final-lepton transverse-momentum distribution normalized by σ_{SM}: Tevatron energy $\sqrt{s} = 1.96$ TeV.

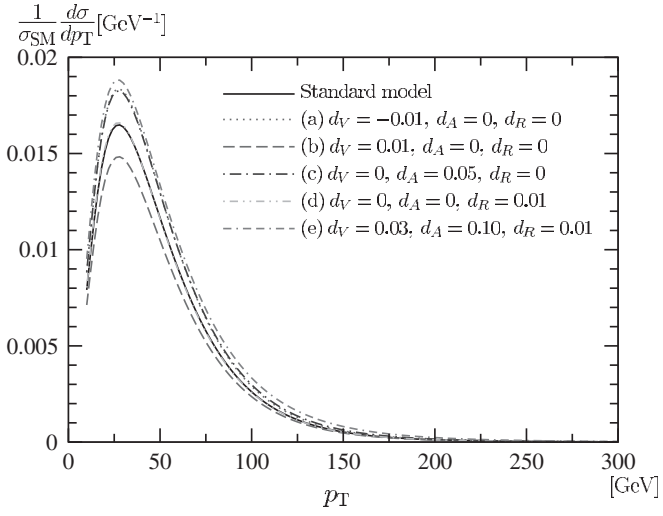

FIG. 8. The final-lepton transverse-momentum distribution normalized by σ_{SM}: LHC energy $\sqrt{s} = 7$ TeV.

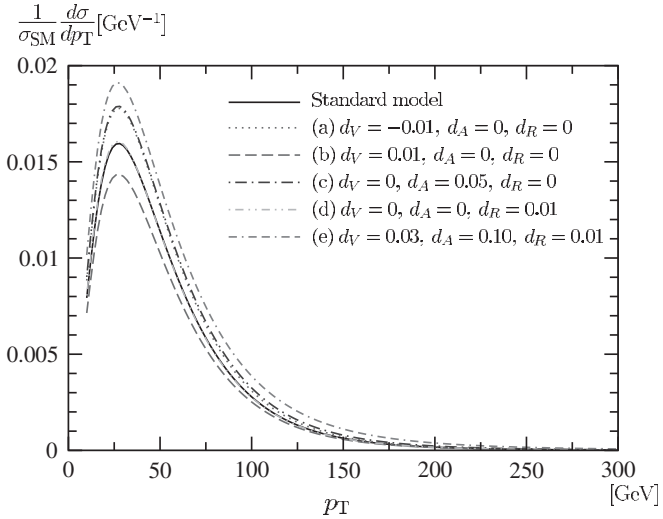

FIG. 9. The final-lepton transverse-momentum distribution normalized by σ_{SM}: LHC energy $\sqrt{s} = 14$ TeV.

distributions around their peak points. The size of the deviations in percentage at $p_T = 50$ GeV is as follows:
Tevatron

$$\begin{aligned} \delta(\mathrm{a}) &= +9.48\%, \qquad \delta(\mathrm{b}) = -8.94\%, \\ \delta(\mathrm{c}) &= +2.14\%, \qquad \delta(\mathrm{d}) = -0.49\%, \\ \delta(\mathrm{e}) &= -17.42\%. \end{aligned} \tag{53}$$

LHC (7 TeV)

$$\begin{aligned} \delta(\mathrm{a}) &= +11.34\%, \qquad \delta(\mathrm{b}) = -10.03\%, \\ \delta(\mathrm{c}) &= +11.08\%, \qquad \delta(\mathrm{d}) = -0.39\%, \\ \delta(\mathrm{e}) &= +14.60\%. \end{aligned} \tag{54}$$

LHC (14 TeV)

$$\begin{aligned} \delta(\mathrm{a}) &= +11.45\%, \qquad \delta(\mathrm{b}) = -10.02\%, \\ \delta(\mathrm{c}) &= +12.63\%, \qquad \delta(\mathrm{d}) = -0.34\%, \\ \delta(\mathrm{e}) &= +20.97\%. \end{aligned} \tag{55}$$

V. SUMMARY AND REMARKS

We have studied possible anomalous $t\bar{t}g$-, $t\bar{t}gg$-, and tbW-interaction effects in the final-lepton distributions of $p\bar{p}/pp \to t\bar{t}X \to \ell^+X'$ at Tevatron and LHC by assuming that there exists a new physics characterized by an energy scale Λ, and we only have standard-model particles/fields below Λ. Under this assumption, all leading anomalous interactions are given by dimension-6 effective operators [2,4,5]. Based on the interaction Lagrangians composed of relevant effective operators, we have derived analytical formulas of the parton-level cross sections of the processes $q\bar{q}/gg \to t\bar{t}X \to \ell^+X'$ *for the first time including both anomalous CP-conserving and CP-violating top-gluon couplings as well as anomalous tbW couplings at the same time*.[3] We then performed numerical calculations for the hadron-level processes at Tevatron and LHC experiments. The results were shown in Figs. 1–9, and then we came to the following conclusions:

(i) In case of $d_V \neq 0$ and $d_A \simeq 0$, we could observe discrepancy between the SM prediction and those with nonstandard effects. Moreover, comparing shapes depicted using parameter sets (a) and (b) in all figures, we saw that the opposite sign of d_V could induce opposite deviation from the SM predictions. This is simply because the leading d_V contribution comes from its linear terms, which fact will however be useful for determining the sign of this parameter.

(ii) If both d_V and d_A are not so small, some nonstandard effects are expected to be observed. Furthermore, they could appear as different corrections at Tevatron and LHC: Look at Figs. 4 and 5, for example. We see that deviations induced by parameter set (e) for Tevatron and LHC are in opposite direction from the SM prediction each other. The same holds true for other figures shown here. Those different deviations originate from the difference in the $t\bar{t}$-production mechanisms at Tevatron and LHC, i.e., $q\bar{q}$-annihilation processes are dominant at Tevatron, while gluon-fusion processes dominate at LHC. This shows that Tevatron and LHC work complementarily to each other.

[3]A similar work was done for the same processes (but in a different formalism) in [13], where anomalous *CP*-violating top-gluon couplings and anomalous *tbW* couplings were taken into account.

(iii) In contrast to those $d_{V,A}$ contributions, that from d_R was found to produce no sizable effects in the distributions we calculated here, and therefore it is difficult to measure its contributions in the processes on which we focused.

Finally, let us close this section with a couple of remarks. First, we have limited our anomalous-coupling values to the inside of the allowed region given in the Appendix (Fig. 10). However this constraint reflects 1σ level uncertainties. That is, their true values might be outside that region, which leads to the possibility that larger deviations from the SM prediction could be observed. Second, we expressed all the anomalous interactions in terms of several constant parameters. This is justified only when $\sqrt{\hat{s}} \ll \Lambda$ holds, which assumption might become less accurate with increasing center-of-mass energy of LHC if the new physics is just around the corner. In that case, unexpected nonstandard effects could be measured. Therefore, even if we might not discover any new particles at LHC, it must be meaningful and important to increase its energy in order to get signals from new physics beyond the standard model. At any rate, we believe what was presented here will be one of the most promising approaches to new physics at Tevatron and the current energy scale of LHC ($\sqrt{s} = 7$ TeV).

ACKNOWLEDGMENTS

This work originates in part the doctor thesis of K. O. on CP violation in $p\bar{p} \to t\bar{t}$ and an encouraging comment to it by Bohdan Grzadkowski about taking into account the final lepton, which comment we appreciate very much. This is partly supported by the Grant-in-Aid for Scientific Research No. 22540284 from the Japan Society for the Promotion of Science. The algebraic calculations using FORM were carried out on the computer system at Yukawa Institute for Theoretical Physics (YITP), Kyoto University.

APPENDIX: CONSTRAINTS ON THE ANOMALOUS TOP-GLUON COUPLINGS

In our previous analysis on d_V and d_A through the total cross section of $t\bar{t}$ productions [6], we pointed out that LHC data could give a stronger constraint on them, which would be hard to obtain from Tevatron data alone. We then showed in [7] that the first CMS measurement of this quantity [18] actually made it possible. That is, we have obtained a stronger constraint on $d_{V,A}$ by combining the CDF/D0 data [17]

$$\sigma_{\rm exp} = 7.02 \pm 0.63 \text{ pb} \qquad (\text{CDF: } m_t = 175 \text{ GeV}) \tag{A1}$$

$$= 8.18^{+0.98}_{-0.87} \text{ pb} \quad (\text{D0: } m_t = 170 \text{ GeV}) \tag{A2}$$

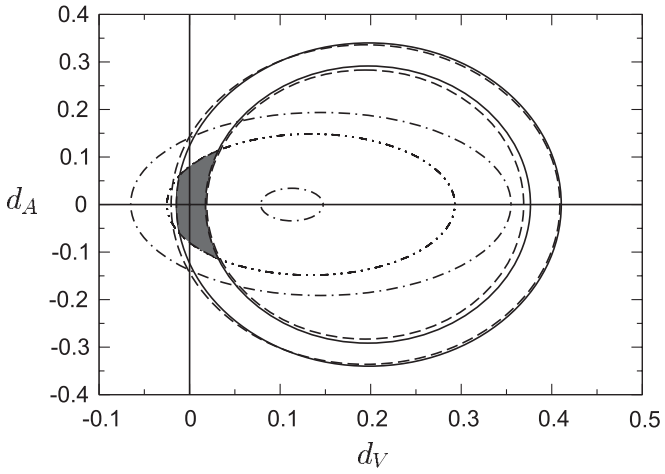

FIG. 10. The $d_{V,A}$ region allowed by Tevatron and LHC data altogether (the shaded part). The solid curves, the dashed curves and the dash-dotted curves are, respectively, from CDF, D0 and CMS data, and the dash-dot-dotted curve is from ATLAS data.

with the CMS data

$$\sigma_{\rm exp} = 194 \pm 72(\text{stat}) \pm 24(\text{syst}) \pm 21(\text{lumi}) \text{ pb} \quad (m_t = 172.5 \text{ GeV}) \tag{A3}$$

than in the analysis with the above CDF/D0 data alone. Since we now also have ATLAS data [19]

$$\sigma_{\rm exp} = 145 \pm 31^{+42}_{-27} \text{ pb} \qquad (m_t = 172.5 \text{ GeV}), \tag{A4}$$

where the first uncertainty is statistical and the second systematic, it is worth carrying out the same analysis again with all the data available here.[4]

In this analysis, we need the absolute value of the cross section, for which we cannot neglect the QCD radiative corrections. As for such corrected SM contribution, we took the next-to-leading-order (NLO) cross section

$$\sigma^{\rm NLO}_{\rm SM} = 157.5^{+23.2}_{-24.4} \text{ pb} \tag{A5}$$

in [7], which was used by the CMS [18]. We here, however, take account of the NNLO value

$$\sigma^{\rm NNLO}_{\rm SM} = 164.6^{+11.4}_{-15.7} \text{ pb} \qquad (m_t = 172.5 \text{ GeV}) \tag{A6}$$

as in [19].

The result is shown in Fig. 10, where the shaded part is the $d_{V,A}$ region allowed by Tevatron and LHC data altogether. There does not seem to be any big difference from the result in [7], but the allowed area has become a bit narrower by adding the ATLAS data. All the parameter values used in the main text were taken from inside this region.

[4]We do not repeat describing the detail of the calculations here and leave it to [6].

[1] LHC Web site: http://public.web.cern.ch/public/en/LHC/LHC-en.html.

[2] W. Buchmuller and D. Wyler, Nucl. Phys. B **268**, 621 (1986); C. Arzt, M. B. Einhorn, and J. Wudka, Nucl. Phys. B **433**, 41 (1995).

[3] B. Grzadkowski, Z. Hioki, K. Ohkuma, and J. Wudka, Nucl. Phys. B **689**, 108 (2004).

[4] J. A. Aguilar-Saavedra, Nucl. Phys. B **812**, 181 (2009); **821**, 215 (2009).

[5] B. Grzadkowski, M. Iskrzynski, M. Misiak, and J. Rosiek, J. High Energy Phys. 10 (2010) 085.

[6] Z. Hioki and K. Ohkuma, Eur. Phys. J. C **65**, 127 (2010).

[7] Z. Hioki and K. Ohkuma, Eur. Phys. J. C **71**, 1535 (2011).

[8] A. Brandenburg and J. P. Ma, Phys. Lett. B **298**, 211 (1993).

[9] P. Haberl, O. Nachtmann, and A. Wilch, Phys. Rev. D **53**, 4875 (1996).

[10] K. m. Cheung, Phys. Rev. D **53**, 3604 (1996); **55**, 4430 (1997).

[11] B. Grzadkowski, B. Lampe, and K. J. Abraham, Phys. Lett. B **415**, 193 (1997).

[12] B. Lampe, Phys. Lett. B **415**, 63 (1997).

[13] O. Antipin and G. Valencia, Phys. Rev. D **79**, 013013 (2009).

[14] S. K. Gupta, A. S. Mete, and G. Valencia, Phys. Rev. D **80**, 034013 (2009).

[15] S. K. Gupta and G. Valencia, Phys. Rev. D **81**, 034013 (2010).

[16] C. Zhang and S. Willenbrock, Phys. Rev. D **83**, 034006 (2011).

[17] CDF collaboration: Public CDF note Report No. 9448, http://www-cdf.fnal.gov/physics/new/top/public_xsection.html; V. M. Abazov *et al.* (D0 Collaboration), Phys. Rev. D **80**, 071102 (2009).

[18] V. Khachatryan *et al.* (CMS Collaboration), Phys. Lett. B **695**, 424 (2011).

[19] G. Aad *et al.* (The ATLAS Collaboration), Eur. Phys. J. C **71**, 1577 (2011).

[20] S. Kawasaki, T. Shirafuji, and S. Y. Tsai, Prog. Theor. Phys. **49**, 1656 (1973).

[21] Y. S. Tsai, Phys. Rev. D **4**, 2821 (1971); **13**, 771 (1976).

[22] D. Berdine, N. Kauer, and D. Rainwater, Phys. Rev. Lett. **99**, 111601 (2007); N. Kauer, Phys. Lett. B **649**, 413 (2007); C. F. Uhlemann and N. Kauer, Nucl. Phys. B **814**, 195 (2009).

[23] Particle Data Group Web site (The Review of Particle Physics), http://pdg.lbl.gov/.

[24] V. M. Abazov *et al.* (D0 Collaboration), Phys. Rev. Lett. **106**, 022001 (2011); T. Aaltonen *et al.* (CDF Collaboration), Phys. Rev. Lett. **105**, 232003 (2010).

[25] T. Aaltonen *et al.* (CDF Collaboration), Phys. Rev. D **82**, 112005 (2010).

[26] V. M. Abazov *et al.* (D0 Collaboration), Phys. Rev. Lett. **101**, 221801 (2008); , **102**, 092002 (2009); , Phys. Rev. D **83**, 032009 (2011).

[27] T. Aaltonen *et al.* (CDF Collaboration), Phys. Rev. Lett. **105**, 042002 (2010).

[28] T. Arens and L. M. Sehgal, Phys. Rev. D **50**, 4372 (1994).

[29] The Tevatron Electroweak Working Group, for the CDF Collaboration and the D0 Collaboration, arXiv:0808.1089.

[30] B. Grzadkowski and Z. Hioki, Phys. Lett. B **476**, 87 (2000); **529**, 82 (2002); **557**, 55 (2003).

[31] S. D. Rindani, Pramana **54**, 791 (2000).

[32] R. M. Godbole, S. D. Rindani, and R. K. Singh, J. High Energy Phys. 12 (2006) 021.

[33] P. M. Nadolsky *et al.*, Phys. Rev. D **78**, 013004 (2008).

[34] G. Bevilacqua, M. Czakon, A. van Hameren, C. G. Papadopoulos, and M. Worek, J. High Energy Phys. 02 (2011) 083.

[35] R. Frederix and F. Maltoni, J. High Energy Phys. 01 (2009) 047.